

selective conductance—for example, in the case of the KcsA or gramicidin channels, by provision of multiple oriented carbonyl groups that each carry a  $\delta^-$  charge, within narrow selective regions. These can replace or compensate for waters that are displaced from the first hydration shell (32–36).

Removal of water from, and fixation of a specific conformation of glycerol in the GlpF channel are also energetically costly processes. The channel achieves selectivity and conductance by provision of an amphipathic pathway that closely matches successive CH-OH groups. In GlpF, polar interactions are only possible on one side of the conducting pathway, and the hydration shell around an ion cannot be compensated for at all on the hydrophobic side. Consequently, all ions including OH<sup>-</sup>, or H<sub>3</sub>O<sup>+</sup>, are excluded from the channel. By also requiring a permeant group that is polarizable with both  $\delta^+$  donor, and  $\delta^-$  acceptor, characteristics at each position in the selectivity filter, carbohydrates composed of CH-OH moieties are efficiently transported. Thus, the structure shows the precise mechanism for sharp selectivity and high conductance of alditols while excluding all charged species and water.

#### References and Notes

- G. M. Preston *et al.*, *Science* **256**, 385 (1992).
- C. Maurel *et al.*, *J. Biol. Chem.* **269**, 11869 (1994).
- J. H. Park, M. H. Saier Jr., *J. Membr. Biol.* **153**, 171 (1996).
- A. Finkelstein, *Water Movement Through Lipid Bilayers, Pores, and Plasma Membranes: Theory and Reality* (Wiley, New York, 1987).
- K. B. Heller, E. C. Lin, T. H. Wilson, *J. Bacteriol.* **144**, 274 (1980).
- G. M. Pao *et al.*, *Mol. Microbiol.* **5**, 33 (1991).
- G. J. Wistow, M. M. Pisano, A. B. Chepelinsky, *Trends Biochem. Sci.* **16**, 170 (1991).
- T. L. Anthony *et al.*, *Mol. Pharmacol.* **57**, 576 (2000).
- A. Engel, Y. Fujiyoshi, P. Agre, *EMBO J.* **19**, 800 (2000).
- B. L. Smith, P. Agre, *J. Biol. Chem.* **266**, 6407 (1991).
- A. Cheng *et al.*, *Nature* **387**, 627 (1997).
- H. Li, S. Lee, B. K. Jap, *Nature Struct. Biol.* **4**, 263 (1997).
- L. Hasler *et al.*, *J. Mol. Biol.* **279**, 855 (1998).
- P. Ringle *et al.*, *J. Mol. Biol.* **291**, 1181 (1999).
- T. Walz *et al.*, *Nature* **387**, 624 (1997).
- K. Mitsuoka *et al.*, *J. Struct. Biol.* **128**, 34 (1999).
- J. B. Heymann, A. Engel, *J. Mol. Biol.* **295**, 1039 (2000).
- C. Maurel, J. Reizer, J. I. Schroeder, M. J. Chrispeels, *EMBO J.* **12**, 2241 (1993).
- D. Walther, F. Eisenhaber, P. Argos, *J. Mol. Biol.* **255**, 536 (1996).
- G. M. Preston *et al.*, *Science* **265**, 1585 (1994).
- M. M. Javadpour *et al.*, *Biophys. J.* **77**, 1609 (1999).
- P. Lauger, H. J. Apell, *Biophys. Chem.* **16**, 209 (1982).
- V. Lagree *et al.*, *J. Biol. Chem.* **273**, 12422 (1998).
- J. D. Bernal, R. H. Fowler, *J. Chem. Phys.* **1**, 515 (1933).
- D. Eisenberg, W. Kauzman, *The Structure and Properties of Water* (Oxford Univ. Press, London, 1969).
- G. V. Prasad *et al.*, *J. Biol. Chem.* **273**, 33123 (1998).
- M. J. Borgnia *et al.*, *J. Mol. Biol.* **291**, 1169 (1999).
- P. M. Deen *et al.*, *J. Clin. Invest.* **95**, 2291 (1995).
- A. J. Yool, W. D. Stamer, J. W. Regan, *Science* **273**, 1216 (1996).
- M. Yasui *et al.*, *Nature* **402**, 184 (1999).
- O. S. Andersen, R. E. d. Koeppe, *Physiol. Rev.* **72**, S89 (1992).
- L. J. Mullins, *J. Gen. Physiol.* **42**, 817 (1959).
- D. A. Doyle, B. A. Wallace, *J. Mol. Biol.* **266**, 963 (1997).
- D. A. Doyle *et al.*, *Science* **280**, 69 (1998).
- G. Chang *et al.*, *Science* **282**, 2220 (1998).
- B. Roux, R. MacKinnon, *Science* **285**, 100 (1999).
- CCP4, *Acta Crystallogr. D* **50**, 760 (1994).
- E. LaFortelle, J. J. Irwin, G. Bricogne, in *Crystallographic Computing 7*, P. Bourne, K. D. Watenpaugh, Eds. (Oxford Univ. Press, London, 1997).
- A. T. Brünger, *X-PLOR Version 3.843* (Yale University, New Haven, CT, 1996).
- N. Guex, M. C. Peitsch, *Electrophoresis* **18**, 2714 (1997).
- <http://www.povray.org>
- F. Szoka Jr., D. Papahadjopoulos, *Annu. Rev. Biophys. Bioeng.* **9**, 467 (1980).
- P. C. Maloney, S. V. Ambudkar, *Arch. Biochem. Biophys.* **269**, 1 (1989).
- P. Agre *et al.*, *Methods Enzymol.* **294**, 550 (1999).
- We thank T. Earnest for help and support at the Advanced Light Source (ALS), Lawrence Berkeley National Laboratory, J. Newdoll ([www.brushwithscience.com](http://www.brushwithscience.com)) for help with figure preparation and text, and J. Finer Moore for advice. We also thank D. Akhavan for help with Table 2 and S. Sine and P. Maloney for discussions. Supported by NIH grant GM24485 (R.M.S.). D.F. and A.L. received postdoctoral support from NIH. P.N. received postdoctoral support from the Human Frontiers Research Science Organization (grant LT0156/1999-M). Coordinates of the structure have been deposited in the Research Collaboratory for Structural Bioinformatics (RCSB) Protein Data Bank (accession code 1FX8).

11 May 2000; accepted 25 September 2000

## Control of Viremia and Prevention of Clinical AIDS in Rhesus Monkeys by Cytokine-Augmented DNA Vaccination

Dan H. Barouch,<sup>1\*</sup> Sampa Santra,<sup>1</sup> Jörn E. Schmitz,<sup>1</sup> Marcelo J. Kuroda,<sup>1</sup> Tong-Ming Fu,<sup>2</sup> Wendeline Wagner,<sup>3</sup> Mirosława Bilśka,<sup>4</sup> Abie Craiu,<sup>1</sup> Xin Xiao Zheng,<sup>1</sup> Georgia R. Krivulka,<sup>1</sup> Kristin Beaudry,<sup>1</sup> Michelle A. Lifton,<sup>1</sup> Christine E. Nickerson,<sup>1</sup> Wendy L. Trigona,<sup>2</sup> Kara Punt,<sup>2</sup> Dan C. Freed,<sup>2</sup> Liming Guan,<sup>2</sup> Sheri Dubey,<sup>2</sup> Danilo Casimiro,<sup>2</sup> Adam Simon,<sup>2</sup> Mary-Ellen Davies,<sup>2</sup> Michael Chastain,<sup>2</sup> Terry B. Strom,<sup>1</sup> Rebecca S. Gelman,<sup>5</sup> David C. Montefiori,<sup>4</sup> Mark G. Lewis,<sup>3</sup> Emilio A. Emini,<sup>2</sup> John W. Shiver,<sup>2</sup> Norman L. Letvin<sup>1</sup>

With accumulating evidence indicating the importance of cytotoxic T lymphocytes (CTLs) in containing human immunodeficiency virus-1 (HIV-1) replication in infected individuals, strategies are being pursued to elicit virus-specific CTLs with prototype HIV-1 vaccines. Here, we report the protective efficacy of vaccine-elicited immune responses against a pathogenic SHIV-89.6P challenge in rhesus monkeys. Immune responses were elicited by DNA vaccines expressing SIVmac239 Gag and HIV-1 89.6P Env, augmented by the administration of the purified fusion protein IL-2/Ig, consisting of interleukin-2 (IL-2) and the Fc portion of immunoglobulin G (IgG), or a plasmid encoding IL-2/Ig. After SHIV-89.6P infection, sham-vaccinated monkeys developed weak CTL responses, rapid loss of CD4<sup>+</sup> T cells, no virus-specific CD4<sup>+</sup> T cell responses, high setpoint viral loads, significant clinical disease progression, and death in half of the animals by day 140 after challenge. In contrast, all monkeys that received the DNA vaccines augmented with IL-2/Ig were infected, but demonstrated potent secondary CTL responses, stable CD4<sup>+</sup> T cell counts, preserved virus-specific CD4<sup>+</sup> T cell responses, low to undetectable setpoint viral loads, and no evidence of clinical disease or mortality by day 140 after challenge.

Recent studies have demonstrated the critical role of virus-specific CD8<sup>+</sup> CTL responses in controlling HIV-1 replication in humans and simian immunodeficiency virus (SIV) replication in rhesus monkeys (1–5). It is therefore widely believed that candidate HIV-1 vaccines should elicit potent virus-specific CTL responses. Plasmid DNA vaccination is capable of eliciting both humoral and cellular immune responses (6–8). DNA vaccine-elicited immune responses have pro-

tected nonhuman primates against challenges with nonpathogenic AIDS viruses (9, 10) and have afforded a degree of protection against pathogenic viral challenges (11, 12).

Boosting a DNA-primed immune response with a live recombinant vector has been shown to augment CTL responses and confer control of nonpathogenic viral challenges (13–16). Plasmid IL-2 has also been shown to augment DNA vaccine-elicited immune responses in a variety of murine disease

RESEARCH ARTICLES

models (17–19). We extended these observations by investigating the vaccine adjuvant properties of IL-2/Ig, a fusion protein consisting of IL-2 and the Fc portion of IgG. This fusion protein has IL-2 functional activity as well as the advantages of divalent avidity and a long in vivo half-life (20, 21).

We previously reported that a plasmid encoding murine IL-2/Ig was able to augment CTL and antibody responses elicited by an HIV-1 gp120 DNA vaccine in mice (22). We have also demonstrated that administration of human IL-2/Ig, either as a protein or a plasmid, markedly augmented DNA vaccine-elicited HIV-1- and SIV-specific immune responses in rhesus monkeys (23). Here, we report that the immunity elicited by IL-2/Ig-augmented DNA vaccines confers control of a highly pathogenic SHIV-89.6P viral challenge.

Vaccine-elicited immune responses.

Twenty rhesus monkeys (*Macaca mulatta*) were immunized with a sham pV1R plasmid ( $n = 8$ ), SIVmac239 Gag and HIV-1 89.6P Env DNA vaccines alone ( $n = 4$ ), or these DNA vaccines plus IL-2/Ig ( $n = 8$ ) (Fig. 1A) (24). The plasmid DNA vaccines expressed genes optimized for high-level expression and used a cytomegalovirus promoter in a pV1R vector backbone. The IL-2/Ig was administered as purified human IL-2/Ig protein in four animals or as a plasmid expressing human IL-2/Ig in four animals. The immune responses elicited by the initial immunizations have been described (23).

In the 15 rhesus monkeys included in this study that expressed the major histocompatibility complex (MHC) class I allele *Mamu-A\*01*, we measured vaccine-elicited CTL responses specific for the *Mamu-A\*01*-restricted immunodominant SIV Gag p11C (CTPY-DINQM) and subdominant HIV-1 Env p41A (YAPPISGQI) epitopes (25–28). After the final immunization at week 40, the vaccinated monkeys developed significant circulating p11C- and p41A-specific CD8<sup>+</sup> T lymphocytes detected by tetramer staining (Fig. 1, B and C) (29, 30). In contrast, the control monkeys had no detectable circulating tetramer-positive CD8<sup>+</sup> T lymphocytes. Moreover, as expected, since these animals were not vaccinated with an SIV Pol immunogen, none of the monkeys had detectable tetramer-positive CD8<sup>+</sup> T lymphocytes specific for the *Mamu-A\*01*-restricted SIV Pol p68A epitope (STP-

PLVRLV) (31). Functional chromium release cytotoxicity assays were also performed with the p11C, p41A, and p68A epitope peptides and

corroborated these results (31). The monkeys that received the DNA vaccines plus IL-2/Ig protein or IL-2/Ig plasmid demonstrated mark-

**Fig. 1.** Vaccine trial design and prechallenge CTL responses. (A) Monkeys were immunized as shown at weeks 0, 4, 8, and 40 with the SIVmac239 Gag and HIV-1 Env 89.6P DNA vaccines (24). At weeks 0 and 4, certain monkeys also received IL-2/Ig protein or IL-2/Ig plasmid (arrows with circles). At weeks 8 and 40, all monkeys received only the DNA vaccines (arrows without circles). At week 46, all monkeys were challenged with 100 MID<sub>50</sub> SHIV-89.6P by the intravenous route (long arrow). Vaccine-elicited CD8<sup>+</sup> T cell responses specific for the *Mamu-A\*01*-restricted (B) SIV Gag p11C (CTPY-DINQM) and (C) HIV-1 Env p41A (YAPPISGQI) epitopes were measured in the *Mamu-A\*01*-positive monkeys by tetramer staining. Freshly isolated PBMCs were stained directly ex vivo with fluorochrome-labeled *Mamu-A\*01*/p11C or *Mamu-A\*01*/p41A tetramers as described (30). Percent CD3<sup>+</sup>CD8<sup>+</sup> T cells that bound each tetramer are shown. Means and standard errors for each group are shown.

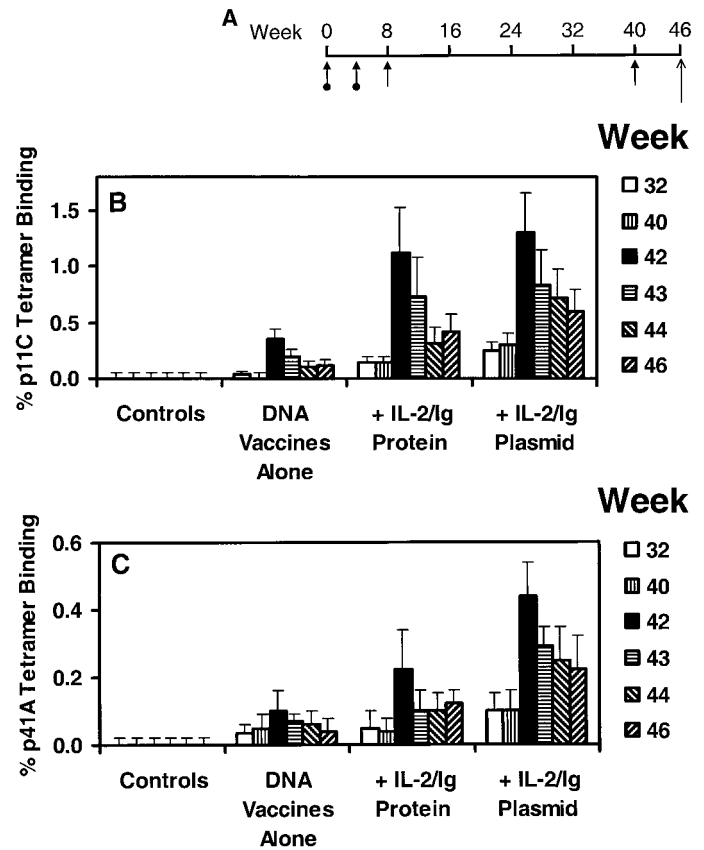


**Table 1.** Analysis of CD8<sup>+</sup> T cell responses in the *Mamu-A\*01*-positive monkeys by tetramer staining of freshly isolated PBMCs, tetramer staining of peptide-stimulated PBMCs, and functional chromium release cytotoxicity assays with peptide-stimulated PBMCs on day 63 after challenge (23, 30). Percent CD3<sup>+</sup>CD8<sup>+</sup> cells that bind tetramer are shown for the tetramer assays. Percent-specific lysis at a 5:1 effector-to-target ratio are shown for the cytotoxicity assays.

Monkey	Tetramer binding (fresh PBMCs)			Tetramer binding (stimulated PBMCs)			Cytotoxicity assay (stimulated PBMCs)		
	p11C	p41A	p68A	p11C	p41A	p68A	p11C	p41A	p68A
<i>Controls</i>									
KPB	0.2	0	0.1	1	0	0	3	0	0
KPE	0.8	0	0.1	17	0	1	14	0	0
PKT	0.1	0.1	0	1	0	0	0	0	0
TDE	0.2	0	0	2	1	0	0	0	0
<i>DNA vaccines alone</i>									
702	1.5	0.1	0	27	21	1	35	32	2
811	7.9	0	0	14	1	0	14	0	0
820	1.3	0	0.1	18	1	3	16	0	2
<i>DNA + IL-2/Ig protein</i>									
712	2.9	0.1	0.1	72	11	4	49	8	3
772	4.4	0.3	0.1	59	28	18	49	26	11
798	3.1	0.3	0.2	63	39	19	43	20	12
839	2.2	0.3	0.1	49	10	4	39	11	2
<i>DNA + IL-2/Ig plasmid</i>									
483	5.1	0.4	0.1	88	74	3	55	55	4
728	3.5	0.3	0.1	63	16	8	46	29	2
833	3.0	0.2	0.1	59	22	2	43	19	2
893	4.1	0.5	0.3	86	75	65	54	48	52

<sup>1</sup>Department of Medicine, Beth Israel Deaconess Medical Center, Harvard Medical School, 330 Brookline Avenue, Boston, MA 02215, USA. <sup>2</sup>Merck Research Laboratories, West Point, PA 19486, USA. <sup>3</sup>Southern Research Institute, 431 Aviation Way, Frederick, MD 21701, USA. <sup>4</sup>Duke University Medical Center, Durham, NC 27710, USA. <sup>5</sup>Department of Biostatistical Science, Dana-Farber Cancer Institute, 44 Binney Street, Boston, MA 02115, USA.

\*To whom correspondence should be addressed. E-mail: dan\_barouch@hotmail.com

## RESEARCH ARTICLES

edly augmented vaccine-elicited CTL responses compared with the animals that received the DNA vaccines alone. Because cytokines were only administered with the week 0 and 4 immunizations, the persistence of these augmented CTL responses through week 46 demonstrates the durability of the enhanced CTL priming achieved 10 months earlier. At the time of peak immunity at week 42, the monkeys that received the DNA vaccines plus IL-2/Ig plasmid had an average of 1.2% of circulating CD3<sup>+</sup>CD8<sup>+</sup> T cells specific for the p11C epitope and 0.5% specific for the p41A epitope. The tetramer-positive CD3<sup>+</sup>CD8<sup>+</sup> T cells declined thereafter and reached plateau levels of 0.5% for p11C and 0.2% for p41A by the time of challenge. No serum SHIV-89.6P-specific

neutralizing antibodies (<1:4 titer) were detected before challenge (31).

**Immune responses after viral challenge.** Six weeks after the final boost immunization, all 20 rhesus monkeys were challenged by the intravenous route with 100 monkey infectious doses (100 MID<sub>50</sub>) of cell-free SHIV-89.6P. This virus was derived by in vivo passage of SHIV-89.6, a chimeric virus consisting of the SIVmac239 backbone and the HIV-1 89.6 envelope gene, which was cloned from a primary patient R5/X4 dual-tropic HIV-1 isolate (32–34).

The postchallenge CTL responses specific for the p11C (Fig. 2A), p41A (31), and p68A (31) epitopes were determined by staining freshly isolated peripheral blood mononucle-

ar cells (PBMCs) with tetrameric Mamu-A\*01/peptide complexes. The kinetics of the postchallenge CTL responses involved an initial rapid expansion phase that reached a peak at day 14 or 17 after challenge and then fell rapidly to steady-state plateau levels. The control monkeys developed primary p11C-specific CTL responses after challenge, reaching a peak of 1 to 4% of circulating CD3<sup>+</sup>CD8<sup>+</sup> T cells. In contrast, dramatic secondary CTL responses specific for p11C, reaching a maximum of 18 to 40% of circulating CD3<sup>+</sup>CD8<sup>+</sup> T cells, were observed in all the animals that received the DNA vaccine plus IL-2/Ig protein or IL-2/Ig plasmid. Intermediate secondary p11C-specific CTL responses were observed in the animals that received the DNA vaccines alone. Augmented secondary CTL responses specific for the p41A epitope were also detected after challenge in the vaccinated monkeys that received IL-2/Ig, but these responses were of a lower magnitude than those specific for p11C (31). Prior to challenge, the p41A-specific CTL responses elicited by DNA vaccination were only 2.5-fold lower in magnitude than the p11C-specific CTL responses. After challenge, however, the p41A-specific responses were 30-fold lower, reflecting the immunodominance of the p11C CTL epitope in Mamu-A\*01-positive rhesus monkeys in the setting of SHIV infection. As expected, all the monkeys developed weak primary CTL responses specific for the SIV Pol p68A epitope since none of the monkeys were vaccinated with an SIV Pol immunogen (31).

The virus-specific CD8<sup>+</sup> T cell responses were further analyzed by interferon- $\gamma$  (IFN- $\gamma$ ) ELISPOT and intracellular IFN- $\gamma$  staining assays, the results of which correlated well with the results of the tetramer staining (31). Chromium release cytotoxicity assays and tetramer staining of peptide-stimulated PBMCs (23) further corroborated the results of tetramer staining of freshly isolated PBMCs (Table 1).

Neutralizing antibodies (NAbs) were measured in an MT-2 cell-killing assay, using a stock of SHIV-89.6P expanded in human PBMCs as described (35). Detectable NAb titers were measured in 11 of 12 vaccinated monkeys by day 21 after challenge and in two of eight control monkeys (780 and KPE) by day 28 after challenge (Fig. 2B). All animals that developed detectable NAb responses had comparable peak titers.

Six of the eight control monkeys (all except 780 and KPE) demonstrated a rapid and profound depletion of their CD4<sup>+</sup> T lymphocytes between days 7 and 21 after challenge, consistent with our previous experience with SHIV-89.6P infection (Fig. 3A) (33, 34). In contrast, all monkeys that received plasmid DNA vaccines plus IL-2/Ig protein or IL-2/Ig plasmid had complete preservation of their

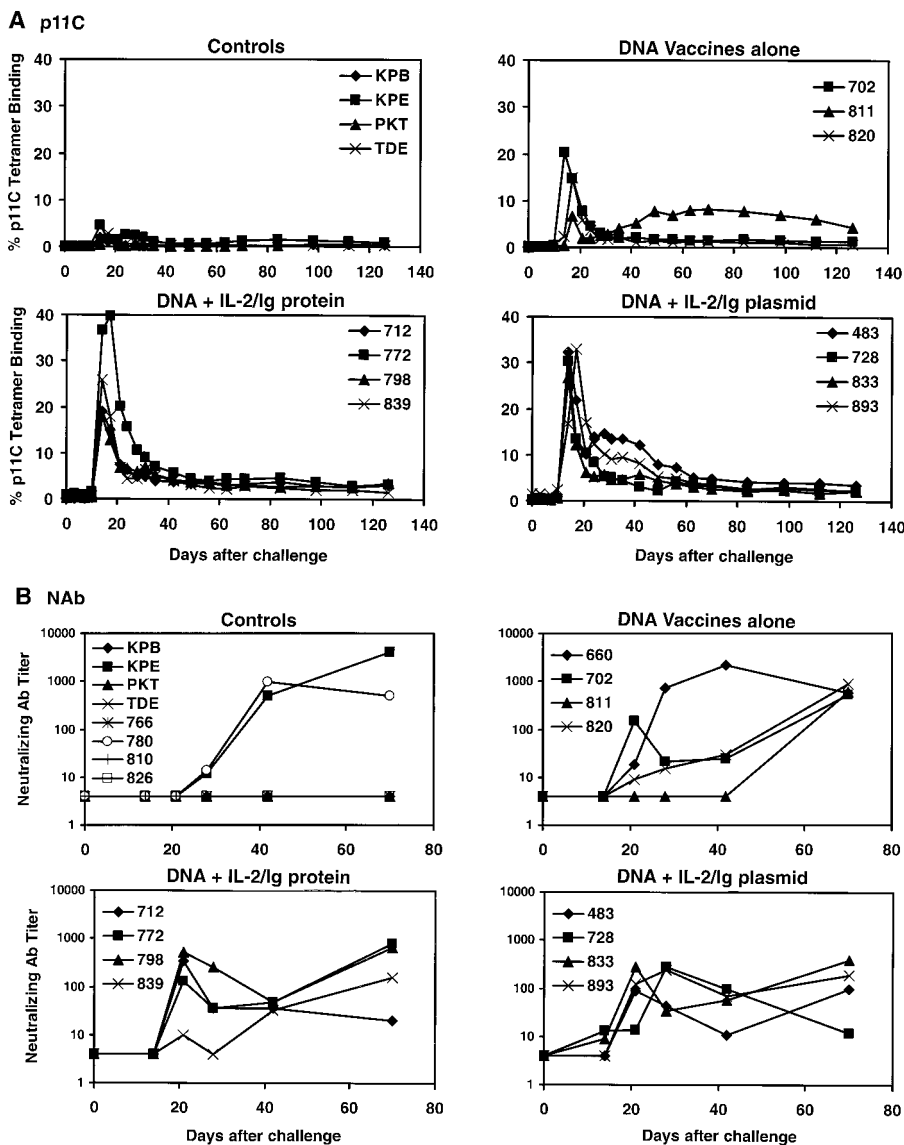


**Fig. 2.** Postchallenge CTL and NAb responses. Monkeys were challenged with SHIV-89.6P by the intravenous route on day 0. (A) In the 15 Mamu-A\*01-positive monkeys, CD8<sup>+</sup> T cell responses specific for the SIV Gag p11C epitope were determined by tetramer binding to freshly isolated PBMCs at multiple time points after challenge (30). Percent CD3<sup>+</sup>CD8<sup>+</sup> T cells that bound the tetramer are shown. (B) In all 20 monkeys, serum antibody titers capable of neutralizing SHIV-89.6P were determined (35).

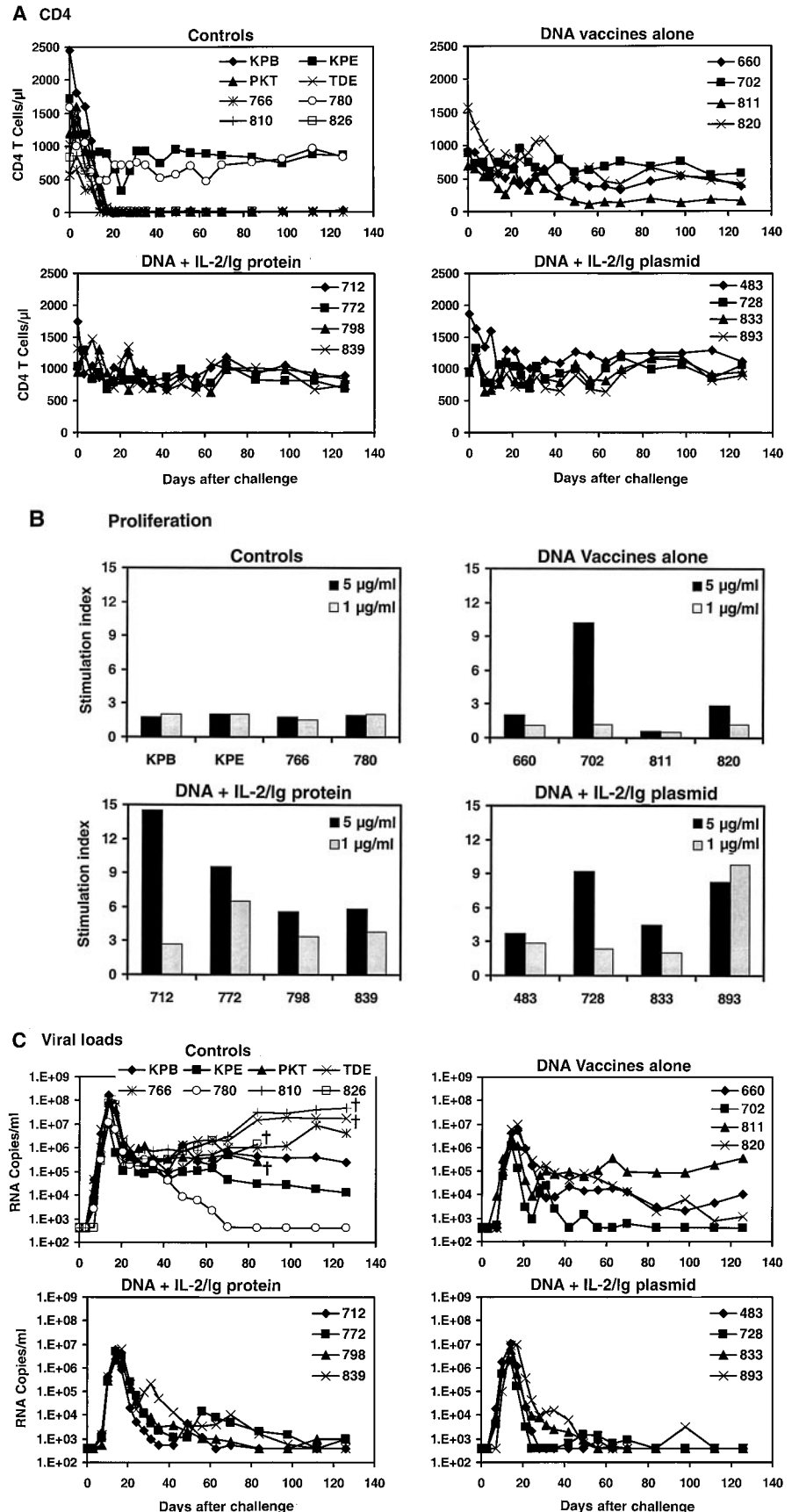
RESEARCH ARTICLES

**Fig. 3.** Postchallenge CD4<sup>+</sup> T lymphocyte counts, virus-specific lymphoproliferative responses, and viral loads. (A) CD4<sup>+</sup> T lymphocyte counts in peripheral blood were determined by multiplying the total lymphocyte count by the percentage of CD3<sup>+</sup>CD4<sup>+</sup> lymphocytes. (B) Lymphoproliferative responses to SIV Gag p28 protein at day 140 after challenge. Standard overnight thymidine incorporation assays were performed after incubation of PBMCs with antigen for 5 days in culture. Stimulation indices were calculated by: (counts per minute with antigen)/(counts per minute with media). (C) Plasma viral loads were determined at multiple time points after challenge by an ultrasensitive branched DNA amplification assay with a detection limit of 400 copies/ml (Bayer Diagnostics). Dagger (†) represents death of the animal.

CD4<sup>+</sup> T lymphocytes, with no evidence of declining CD4<sup>+</sup> T cell counts by day 126 after challenge. At day 70 after challenge, a time by which setpoint of viral replication is reached in SHIV-89.6P-infected rhesus monkeys, a highly significant difference in peripheral blood CD4<sup>+</sup> T cell counts was evident between the control monkeys and the monkeys that received the DNA vaccines plus IL-2/Ig protein or plasmid [*P* = 0.00006, by a two-sided Wilcoxon rank sum test (36)]. The monkeys that received the DNA vaccines alone also had detectable CD4<sup>+</sup> T cell declines, but these were less dramatic than in the control monkeys (*P* = 0.2). In these animals, a marked but gradual CD4<sup>+</sup> T cell decline was observed in monkey 811, and small CD4<sup>+</sup> T cell declines were evident in monkeys 660 and 820.

To determine whether the challenged monkeys retained functional virus-specific CD4<sup>+</sup> T lymphocyte activity, we studied their peripheral blood lymphoproliferative responses after stimulation with purified SIV Gag p28 protein (Intracel) and their CD4<sup>+</sup> T cell IFN-γ responses after stimulation with SIV Gag and HIV-1 Env peptide pools (37). At day 140 after challenge, all the surviving control monkeys, including the monkeys with preserved total CD4<sup>+</sup> T lymphocyte counts (780 and KPE), had no detectable lymphoproliferative responses to SIV Gag (stimulation indices < 2) (Fig. 3B). In contrast, all the monkeys that received the IL-2/Ig-augmented DNA vaccines had detectable lymphoproliferative responses to SIV Gag, with stimulation indices of 3.7 to 14.5. One of the monkeys that received the DNA vaccines alone (monkey 702) also had a detectable lymphoproliferative response. The preservation of virus-specific CD4<sup>+</sup> T lymphocyte function in the vaccinated animals was confirmed by intracellular IFN-γ staining after stimulation with SIV Gag or HIV-1 Env peptide pools (Table 2).

**Viremia and clinical disease progression.** We next measured plasma viral loads in



RESEARCH ARTICLES

the monkeys by an ultrasensitive branched DNA amplification assay with a detection limit of 400 copies/ml (Bayer Diagnostics). The control monkeys had  $1.0 \times 10^7$  to  $1.8 \times 10^8$  copies/ml of virus at the time of peak viremia on day 14 after challenge (Fig. 3C). At day 70 after challenge, six of eight control monkeys had high setpoint viral loads of between  $5.0 \times 10^5$  and  $3.1 \times 10^6$  copies/ml. The other two control monkeys had lower setpoint viral loads:  $4.6 \times 10^4$  copies/ml in monkey KPE and  $4.4 \times 10^2$  copies/ml in monkey 780. In all the vaccinated monkeys, peak viremia was between  $1.2 \times 10^6$  and  $1.0 \times 10^7$  copies/ml, levels significantly lower than in the controls [ $P = 0.004$  and  $P = 0.008$  for monkeys receiving the DNA plus IL-2/Ig or the DNA vaccines alone, respectively, by two-sided Wilcoxon rank-sum tests (36)]. At day 70, setpoint viral loads in the monkeys receiving the IL-2/Ig-augmented DNA vaccines were also significantly lower than in the controls ( $P = 0.004$ ), and a trend toward reduction in setpoint viral loads was evident in the animals that received the DNA vaccines alone ( $P = 0.1$ ). At the majority of time points after setpoint, the monkeys that received the DNA vaccines plus IL-2/Ig plasmid had undetectable viremia (<400 copies/ml), although small and transient rises in viremia were seen in monkeys 728 and 893. In the monkeys that received IL-2/Ig protein, viremia was also generally controlled to under  $10^3$  copies/ml. The monkeys that received the DNA vaccines alone had a heterogeneous outcome, with high setpoint viremia in monkey 811, moderate setpoint viremia in mon-

keys 660 and 820, and controlled viremia in monkey 702.

Compared with the control monkeys, the animals that received the DNA vaccines alone had a 1.9 log reduction in geometric mean viral load after setpoint. The magnitude of this reduction is similar to that seen in previous studies from our laboratory assessing the efficacy of an SIV Gag DNA vaccine (12) or a recombinant MVA-Gag/Pol vaccine (38) in conjunction with SIVsm E660 challenges. The monkeys that received the DNA vaccines plus IL-2/Ig protein or plasmid in the present study had >2.7 and >3.0 log reductions, respectively, in geometric mean viral load after setpoint compared with the control monkeys. In fact, the control of setpoint viremia observed in the monkeys that received the DNA vaccines plus IL-2/Ig plasmid was similar in magnitude to the control of SHIV-89.6P setpoint viremia achieved by immunization with a live, attenuated SIVmac239Δ3 vaccine (39), although the heterologous challenge in that study limits the comparability of results between these reports.

The pathogenicity of the SHIV-89.6P challenge virus was confirmed by the rapid clinical disease progression in the control monkeys that developed low CD4<sup>+</sup> T lymphocyte counts and high viremia. Seven of the eight control monkeys (all except monkey 780) developed significant clinical disease, and four of these eight monkeys died by day 140 after challenge (Fig. 4 and Table 3). In contrast, all monkeys that received the cytokine-augmented DNA vaccines remained healthy with no documented clinical events

or mortality. The prevention of clinical disease in the vaccinated monkeys as compared with the controls was highly significant ( $P = 0.001$ , by a two-sided Fisher exact test), and a trend was observed for preventing mortality ( $P = 0.08$ ). The monkeys that received the DNA vaccines alone had an intermediate clinical outcome, with monkeys 811 and 820 showing signs of clinical disease ( $P = 0.24$  compared with controls).

**Immune correlates of protection.** Scatter plots of data from the *Mamu-A\*01*-positive animals in this study (Fig. 5, A and B) demonstrate significant correlations of prechallenge vaccine-elicited plateau-phase p11C-specific CTL responses determined by tetramer staining, with postchallenge peak p11C-specific CTL responses ( $P = 0.007$ , by a two-sided Spearman rank correlation test) and setpoint viral loads ( $P = 0.04$ ). Levels of peak vaccine-elicited CTLs were less predictive of outcome than those of plateau-phase vaccine-elicited CTLs, the latter presumably reflecting the memory cell population. The asymptotic appearances of the plotted data suggest that a level of vaccine-elicited plateau-phase p11C-specific CTLs may exist (approximately 0.3 to 0.5% of CD3<sup>+</sup>CD8<sup>+</sup> T cells) above which little additional benefit is discernible after challenge. Similar significant correlations were observed between plateau-phase p41A-specific CTL responses before challenge and peak p41A-specific CTL responses and setpoint viral loads after chal-

**Table 2.** Analysis of CD4<sup>+</sup> T cell responses in the surviving monkeys by IFN-γ intracellular staining assays on day 140 after challenge (37). IFN-γ-positive CD4<sup>+</sup> T cells per 10<sup>6</sup> lymphocytes as measured by intracellular IFN-γ staining and flow cytometric analysis are shown in response to media control (Mock), SIV Gag peptide pool, HIV-1 Env peptide pool, and staphylococcal enterotoxin B (SEB). Monkeys 766 and KPB had insufficient CD4<sup>+</sup> T lymphocytes for analysis.

Monkey	IFN-γ-positive CD4 <sup>+</sup> T cells per 10 <sup>6</sup> lymphocytes			
	Mock	SIV Gag	HIV-1 Env	SEB
	<i>Controls</i>			
766	nd	nd	nd	nd
780	167	467	283	20,337
KPB	nd	nd	nd	nd
KPE	228	411	264	12,470
	<i>DNA vaccines alone</i>			
660	142	815	519	18,844
702	161	890	325	44,028
811	142	636	346	nd
820	340	1,121	432	11,869
	<i>DNA + IL-2/Ig protein</i>			
712	164	1,102	410	34,337
772	253	1,353	652	12,352
798	176	1,313	496	3,791
839	141	803	88	14,420
	<i>DNA + IL-2/Ig plasmid</i>			
483	94	1,250	273	26,726
728	287	692	315	9,993
833	172	1,101	358	16,003
893	218	1,540	400	37,406

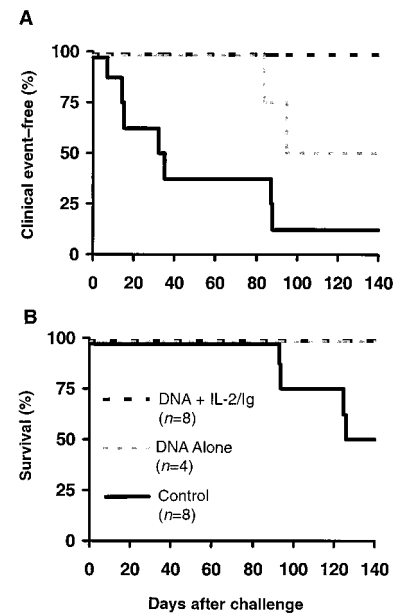


**Fig. 4.** Postchallenge clinical events and mortality in the monkeys that received the cytokine-augmented DNA vaccines, the DNA vaccines alone, or the sham control vaccine. (A) Percentage of monkeys free from clinical events directly attributable to the SHIV-89.6P infection or the subsequent immunodeficiency. (B) Survival curve.

## RESEARCH ARTICLES

lence (31). These results strongly suggest that the improved outcome in animals receiving the cytokine-augmented DNA vaccines resulted from the augmented vaccine-elicited CTL responses in these animals.

No neutralizing antibody (NAb) responses were detected in the vaccinated monkeys prior to challenge, and comparable peak NAb titers developed in the vaccinated monkeys and the two control monkeys with preserved CD4<sup>+</sup> T lymphocyte counts. The other six control monkeys that rapidly lost their CD4<sup>+</sup> T lymphocytes would not be expected to generate significant NAb responses (34). Whereas peak CTL responses occurred on day 14 after challenge, coincident with the peak of primary viremia, NAb responses were generally first detectable on day 21 when viremia had already been partially controlled. The initial control of primary viremia in these monkeys therefore appears to be primarily due to CTL activity, as has previously been observed in HIV-infected humans and SIV-infected monkeys (40–42). However, NAb may also have played a significant role in the control of acute or chronic viremia. In addition, it is possible that IL-2/Ig administration may have modulated nonspecific innate immune functions in these animals and contributed to the containment of virus replication.

**Conclusions.** In summary, after the SHIV-89.6P challenge, 75% of control animals developed weak immune responses, rapid and profound loss of CD4<sup>+</sup> T cells, high viral loads, and rapid disease progression. The *Mamu-A\*01*-positive and the *Mamu-A\*01*-negative control monkeys had similar outcomes, and thus this particular MHC class I allele conferred no particular protective or detrimental effect. It is unclear why monkeys 780 and KPE had more favor-

able outcomes than the other control animals. This may reflect higher virus-specific immune responses or other protective host factors in these animals. The monkeys that received the cytokine-augmented DNA vaccines, in contrast, had uniformly good outcomes with potent immune responses, preserved CD4<sup>+</sup> T cell counts, low to undetectable viral loads, and no evidence of clinical disease. Moreover, these animals also demonstrated preserved virus-specific CD4<sup>+</sup> T cell responses, which may confer long-term clinical benefits (43). The monkeys that received the DNA vaccines alone had intermediate and heterogeneous outcomes. Their postchallenge CTL levels reflected both the levels of prechallenge CTLs as well as the levels of viremia driving these responses.

The administration of IL-2/Ig protein or IL-2/Ig plasmid during initial DNA vaccine priming led to augmented immune responses that were capable of controlling viremia and preventing immunodeficiency, clinical disease, and death following a homologous pathogenic SHIV-89.6P challenge in rhesus monkeys. These results raise the possibility that viral replication may also be reduced in humans who have been similarly vaccinated and subsequently infected with HIV-1. As a consequence, such individuals might manifest decreased disease burden and HIV-1

transmission rates (44, 45). Moreover, this strategy of augmenting vaccine-elicited immune responses by cytokine administration should be readily applicable to other vaccine modalities and for other immunotherapeutic purposes.

### References and Notes

1. A. McMichael, *Cell* **93**, 673 (1998).
2. J. E. Schmitz *et al.*, *Science* **283**, 857 (1999).
3. X. Jin *et al.*, *J. Exp. Med.* **189**, 991 (1999).
4. L. Musey *et al.*, *N. Engl. J. Med.* **337**, 1267 (1997).
5. G. S. Ogg *et al.*, *Science* **279**, 2103 (1998).
6. J. A. Wolff *et al.*, *Science* **247**, 1465 (1990).
7. D. C. Tang, M. Devit, S. A. Johnson, *Nature* **356**, 152 (1992).
8. J. B. Ulmer *et al.*, *Science* **259**, 1745 (1993).
9. N. L. Letvin *et al.*, *Proc. Natl. Acad. Sci. U.S.A.* **94**, 9378 (1997).
10. J. D. Boyer *et al.*, *Nature Med.* **3**, 526 (1997).
11. S. Lu *et al.*, *J. Virol.* **70**, 3978 (1996).
12. M. A. Egan *et al.*, *J. Virol.* **74**, 7485 (2000).
13. H. L. Robinson *et al.*, *Nature Med.* **5**, 526 (1999).
14. S. J. Kent *et al.*, *J. Virol.* **72**, 10180 (1998).
15. T. Hanke *et al.*, *J. Virol.* **73**, 7524 (1999).
16. T. M. Allen *et al.*, *J. Immunol.* **164**, 4968 (2000).
17. M. A. Geissler, A. Gesien, K. Tokushige, J. R. Wands, *J. Immunol.* **158**, 1231 (1997).
18. Y.-H. Chow, W.-L. Huang, W.-K. Chi, Y.-D. Chu, M.-H. Tao, *J. Virol.* **71**, 169 (1997).
19. K.-Q. Xin *et al.*, *Immunology* **94**, 438 (1998).
20. N. F. Landolfi, *J. Immunol.* **146**, 915 (1991).
21. P. Nickerson *et al.*, *Transplant. Immunol.* **4**, 81 (1996).
22. D. H. Barouch *et al.*, *J. Immunol.* **161**, 1875 (1998).
23. D. H. Barouch *et al.*, *Proc. Natl. Acad. Sci. U.S.A.* **97**, 4192 (2000).
24. Large-scale preparations of plasmids were carried out by alkaline lysis and CsCl gradient banding. Rhesus monkeys were vaccinated by intramuscular (i.m.) injections of either 5 mg of HIV-1 89.6P *env* DNA plus 5 mg of SIVmac239 *gag* DNA or 10 mg of sham DNA in sterile saline without adjuvant. Half the dose was delivered to each quadriceps muscle in a 0.5-ml volume using a needle-free Biojector apparatus (Bioject). Monkeys were vaccinated at weeks 0, 4, 8, and 40. At weeks 0 and 4, monkeys that received the DNA vaccines alone also received 5 mg of sham DNA 2 days following vaccination (660, 702, 811, 820); monkeys that received human IL-2/Ig protein received 0.5 mg/day affinity-purified protein in two divided doses i.m. on days 1 through 14 following vaccination (712, 772, 798, 839); and monkeys that received human IL-2/Ig plasmid received 5 mg of IL-2/Ig DNA 2 days following vaccination (483, 728, 833, 893). All the vaccinated monkeys except 660 expressed the *Mamu-A\*01* class I allele. Of the control monkeys, four were *Mamu-A\*01*-negative (766, 780, 810, 826). The four control monkeys that were *Mamu-A\*01*-positive (KPB, KPE, PKT, TDE) were added to the study prior to the week 40 boost immunization. All the animals used in this study were maintained in accordance with the guidelines of the Committee on Animals for Harvard Medical School, the animal care protocols of Southern Research Institute, and the *Guide for the Care and Use of Laboratory Animals* (National Research Council, National Academy Press, Washington, DC, 1996). After challenge, the immunologic assays, viral load measurements, and clinical care of the animals were performed blinded to the immunizations each monkey received.
25. Single-letter abbreviations for the amino acid residues are as follows: A, Ala; C, Cys; D, Asp; G, Gly; I, Ile; L, Leu; M, Met; N, Asn; P, Pro; Q, Gln; R, Arg; S, Ser; T, Thr; V, Val; and Y, Tyr.
26. M. D. Miller, H. Yamamoto, A. H. Hughes, D. I. Watkins, N. L. Letvin, *J. Immunol.* **147**, 320 (1991).
27. T. M. Allen *et al.*, *J. Immunol.* **160**, 6062 (1998). We have simplified previous terminology for the *Mamu-A\*01*-restricted immunodominant SIV Gag epitope from p11C-C-M to p11C for convenience.
28. M. A. Egan *et al.*, *J. Virol.* **73**, 5466 (1999).
29. J. D. Altman *et al.*, *Science* **274**, 94 (1996).
30. M. J. Kuroda *et al.*, *J. Exp. Med.* **187**, 1373 (1998).

**Table 3.** Significant clinical events directly attributable to the SHIV-89.6P infection or the subsequent immunodeficiency in the controls and vaccinated rhesus monkeys through day 140 after challenge.

Monkey	Disease-attributable clinical events
<b>Controls</b>	
766	Chronic cough, wound infection, persistent epistaxis
780	None
810	Chronic diarrhea, persistent epistaxis, rash, weight loss, death
826	Fevers, chronic diarrhea, anorexia, death
KPB	Fevers, persistent epistaxis, chronic diarrhea
KPE	Chronic diarrhea
PKT	Fevers, persistent epistaxis, chronic diarrhea, hematochezia, death
TDE	Explosive diarrhea, weight loss, death
<b>DNA vaccines alone</b>	
660, 702	None
811	Persistent epistaxis, facial swelling/erythema
820	Persistent epistaxis, facial swelling/erythema
<b>DNA + IL-2/Ig protein</b>	
712, 772,	None
798, 839	
<b>DNA + IL-2/Ig plasmid</b>	
483, 728,	None
833, 893	

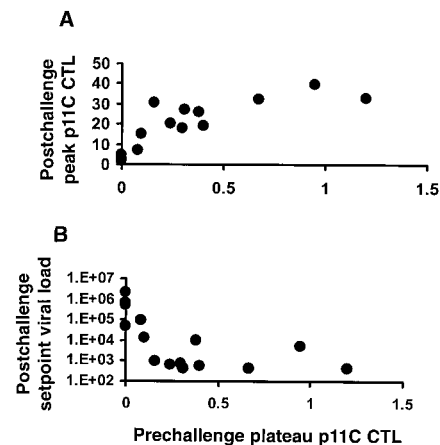


**Fig. 5.** Correlation of prechallenge vaccine-elicited plateau-phase p11C-specific CTL responses as determined by tetramer staining with (A) postchallenge peak p11C-specific CTL responses and (B) setpoint viral loads in the *Mamu-A\*01*-positive rhesus monkeys.

Briefly, 1  $\mu\text{g}$  of phycoerythrin-labeled tetrameric Mamu-A\*01/peptide complexes was used in conjunction with fluorescein isothiocyanate (FITC)-labeled anti-human CD8 $\alpha$  (Leu2a; Becton-Dickinson), ECD-labeled anti-human CD8 $\alpha\beta$  (2ST8-5H7; Beckman Coulter), and APC-labeled anti-rhesus monkey CD3 (FN18; Biosource) monoclonal antibodies to stain peptide-specific CD8 $^+$  T cells. Whole blood (100  $\mu\text{l}$ ) from the vaccinated monkeys was directly stained with these reagents, then lysed, washed, and fixed. Samples were analyzed by four-color flow cytometry on a Coulter EPICS Elite ESP system, and gated CD3 $^+$ CD8 $^+$  T cells were examined for staining with tetrameric Mamu-A\*01/p11C, Mamu-A\*01/p41A, or Mamu-A\*01/p68A complexes.

31. D. H. Barouch *et al.*, data not shown.
32. K. A. Reimann *et al.*, *J. Virol.* **70**, 3198 (1996).
33. K. A. Reimann *et al.*, *J. Virol.* **70**, 6922 (1996).
34. K. A. Reimann *et al.*, *Virology* **256**, 15 (1999).
35. J. M. Crawford *et al.*, *J. Virol.* **73**, 10199 (1999).
36. Statistical analysis was performed with GraphPad Prism, version 2.01 (GraphPad Software, Inc., 1996). CD4 $^+$  T lymphocyte counts and viral loads were compared between groups by two-sided Wilcoxon rank-sum tests with Bonferroni adjustments of  $P$  values to account for the two major comparisons of

each endpoint. Day 70 setpoint values were chosen in order to analyze a complete data set prior to death of any animals. Differences in clinical events and mortality were analyzed by two-sided Fisher exact tests. Correlations of prechallenge vaccine-elicited CTLs and postchallenge peak CTLs or setpoint viral loads were assessed in the vaccinated monkeys by two-sided Spearman rank correlation tests. In all cases,  $P < 0.05$  was considered significant.

37. Intracellular cytokine staining assays were performed as follows. We placed  $2 \times 10^6$  PBMCs in 17 mm by 100 mm polypropylene tubes containing 1 ml of supplemented RPMI medium, to which 1  $\mu\text{g}$  of each costimulatory antibody (anti-CD28 and anti-CD49d, Becton-Dickinson) was added. Peptide pools were added at a final concentration of 2  $\mu\text{g}/\text{ml}$ . Culture tubes were incubated at a 5° slant at 37°C in a humidified 5% CO $_2$  incubator for 16 hours. Brefeldin A (Sigma) was added for the last 15 hours at a final concentration of 10  $\mu\text{g}/\text{ml}$ . Cells were stained with anti-CD3-APC (FN18, Biosource), anti-CD4-PE (OKT4, Ortho Diagnostics), and anti-CD8-PerCP (SK1, Becton-Dickinson) for 30 min and washed with phosphate-buffered saline containing 1% fetal bovine serum. Cells were permeabilized with FACS Permeabilization Buffer (Becton-Dickinson), washed, and

stained with anti-IFN- $\gamma$ -FITC (MD1, Biosource) for 30 min. Samples were fixed in 1% formaldehyde and analyzed on a FACSCalibur flow cytometer (Becton-Dickinson). In order to measure responses of CD4 $^+$  T lymphocytes, 30,000 gated CD3 $^+$ CD4 $^+$  lymphocytes were analyzed for intracellular IFN- $\gamma$  staining events using CellQuest software (Becton-Dickinson).

38. A. Seth *et al.*, *J. Virol.* **74**, 2502 (2000).
39. M. S. Wyand *et al.*, *J. Virol.* **73**, 8356 (1999).
40. R. A. Koup *et al.*, *J. Virol.* **68**, 4650 (1994).
41. G. Pantaleo *et al.*, *Nature* **370**, 463 (1994).
42. Z. W. Chen *et al.*, *J. Exp. Med.* **182**, 21 (1995).
43. E. S. Rosenberg *et al.*, *Science* **278**, 1447 (1997).
44. P. M. Garcia *et al.*, *N. Engl. J. Med.* **341**, 394 (1999).
45. T. C. Quinn *et al.*, *N. Engl. J. Med.* **342**, 921 (2000).
46. We acknowledge support from NIH grants CA-50139 (N.L.L.), AI-85343 (N.L.L. and D.C.M.), AI-65301 (M.G.L.), AI/GF-41521 (T.B.S.), and AI-42298 (T.B.S.). We are grateful to N. Miller, F. Vogel, M. Forman, K. Reimann, W. Lin, A. Miura, R. Kuhnkuhn, C. Lord, J. Frost, T. Steenbeke, C. Crabbs, J. Valley-Ogunro, N. Persaud, L. Zhu, and J. Joyce for generous advice, assistance, and reagents.

4 August 2000; accepted 15 September 2000

## REPORTS

## Imaging Precessional Motion of the Magnetization Vector

Y. Acremann,<sup>1</sup> C. H. Back,<sup>1\*</sup> M. Buess,<sup>1</sup> O. Portmann,<sup>1</sup>  
A. Vaterlaus,<sup>1</sup> D. Pescia,<sup>1</sup> H. Melchior<sup>2</sup>

We report on imaging of three-dimensional precessional orbits of the magnetization vector in a magnetic field by means of a time-resolved vectorial Kerr experiment that measures all three components of the magnetization vector with picosecond resolution. Images of the precessional mode taken with sub-micrometer spatial resolution reveal that the dynamical excitation in this time regime roughly mirrors the symmetry of the underlying equilibrium spin configuration and that its propagation has a non-wavelike character. These results should form the basis for realistic models of the magnetization dynamics in a largely unexplored but technologically increasingly relevant time scale.

A magnetic moment placed at an angle with respect to a magnetic field will feel a torque that tries to align it along the direction of the magnetic field. Because the magnetic moment has an angular momentum, the torque will cause the magnetic moment to precess. This is the content of Larmor's theorem (1). Textbook examples of this theorem are spin resonance phenomena (2–4). Because of its picosecond time scale, precessional motion in ferromagnetic elements attracts technological attention; for instance, precessional magnetization reversal launched by picosecond field pulses has been suggested as a possible way of ad-

vancing the speed of magnetic recording devices into new time scales (5).

This precessional motion has become the target of experiments designed to detect it directly in the time domain (6–11) and, to date, one component of the precessing magnetization vector has been measured accurately with subnanosecond resolution. However, precessional motion evolves in the three-dimensional space defined by the three components of the magnetization vector and is a challenge for direct experimental detection. Yet, measuring all three components as they evolve in time provides essential information necessary to develop realistic models of magnetization dynamics on a picosecond time scale. We explored the vectorial precessional mode launched by a picosecond field pulse in a ferromagnet, which, because of its elementary character, allowed us to directly compare the analytical solution of the Larmor equation with the experimental observations. The result is a

picture of this mode containing unprecedented details that should form the basis for future modeling of this phenomenon.

The sample used here is a flat, polycrystalline Co disk grown by electron-beam evaporation inside a 400-nm-thick, single-turn aluminum coil (see the optical micrograph in Fig. 1A). The Co disk has a diameter of  $\approx 6 \mu\text{m}$  and a thickness of  $\approx 20 \text{ nm}$ , and is capped with  $\approx 2 \text{ nm}$  of Pt for corrosion protection, as the time-resolved experiments are performed at ambient pressure. The magnetic contrast within the Co disk (Fig. 1B) was revealed by spin-polarized scanning electron microscopy (SEMPA) (12). The corresponding domain pattern (summarized schematically in Fig. 1C) shows four in-plane magnetized domains arranged to form a closed magnetic flux configuration within the Co disk, thus minimizing the magnetostatic energy (13). This closed-flux configuration suggests that the shape anisotropy is the essential mechanism establishing the equilibrium spin configuration of Fig. 1B. In our analysis, we neglect other types of magnetic anisotropies, such as the magneto-crystalline one. The simplest mathematical model capturing the symmetry of the closed-flux configuration associates every point in the disk with cylindrical coordinates ( $\rho$ ,  $\varphi$ ,  $z$ ), and assigns cylindrical unit vectors ( $\hat{e}_\rho$ ,  $\hat{e}_\varphi$ ,  $\hat{e}_z$ ) to the magnetization vector ( $M_\rho$ ,  $M_\varphi$ ,  $M_z$ ) = (0,  $M_\varphi$ , 0) (Fig. 1D).

Applying a sudden small magnetic field along  $z$  provides the initial torque which will produce a small but finite  $M_\rho$ . This initial deviation leads to the motion of  $\vec{M}$ , described by the Larmor coupled differential equations (1) [neglecting the product of small terms (3)]

<sup>1</sup>Laboratorium für Festkörperphysik, Eidgenössische Technische Hochschule (ETH) Zürich, CH-8093 Zürich, Switzerland. <sup>2</sup>Institut für Quantenelektronik, ETH Zürich, CH-8093 Zürich, Switzerland.

\*To whom correspondence should be addressed. E-mail: back@solid.phys.ethz.ch